CrossMark

RESEARCH ARTICLE

Hydrogen peroxide sensor based on electrodeposited Prussian blue film

Si-Yuan Lu[1,2] · Yihao Chen[1,2] · Xufei Fang[1,2,3] · Xue Feng[1,2]

Abstract Prussian blue (PB) films have been widely used for blood glucose monitoring. Here, we present the strategy to improve the performance and sensitivity of PB film for hydrogen peroxide (H_2O_2) monitoring by using modified gold electrode for hydrogen peroxide monitoring. The microstructure of the studied electrodes was characterized using scanning electron microscopy and atomic force microscopy. The electrochemical properties of experimental electrodes were obtained via cyclic voltammograms and chronoamperometry methods. The results show that the thickness of deposited PB film is increased with the deposition time. The PB-modified electrode exhibits the widest linear range and best operational stability after being electrochemically deposited for 240 s. The highest sensitivity for experimental electrodes is obtained on samples deposited for 40 s (341 mA cm^{-2} M^{-1}), indicating that a thinner PB film with certain critical thickness can accelerate the exchanging rate of K$^+$ between PB lattice and the tested solution.
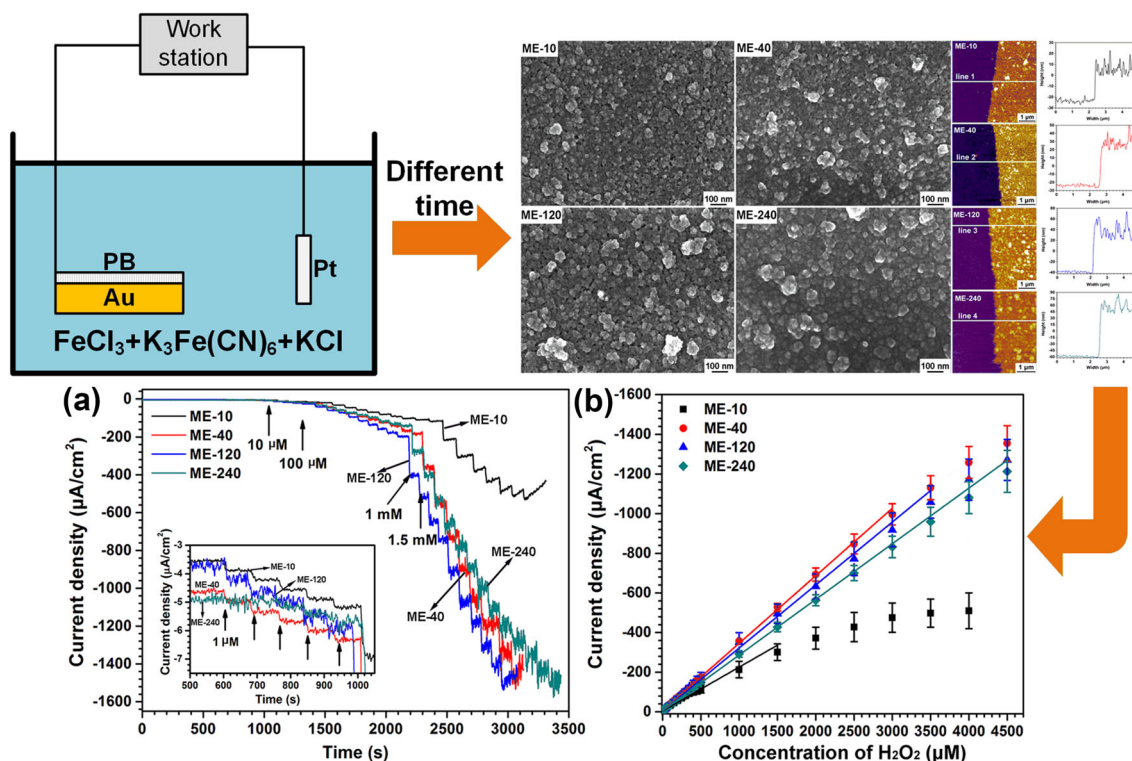
✉ Xue Feng
   fengxue@tsinghua.edu.cn

1   AML, School of Aerospace Engineering, Tsinghua University, Beijing 100084, China

2   Center for Advanced Mechanics and Materials, Tsinghua University, Beijing 100084, China

3   Present Address: Max-Planck-Institut für Eisenforschung GmbH, Max-Planck-Str. 1, 40237 Düsseldorf, Germany

Graphical Abstract

1 Introduction

Hydrogen peroxide (H_2O_2) is the byproduct of several enzymatic processes including glucose oxidase, cholesterol oxidase, and alcohol oxidase. The effective and sensitive detection of H_2O_2 remains of critical importance in analytical field owing to its extensive use in various aspects (e.g., environmental monitoring, pharmaceutical industry, clinical chemistry, and especially the diabetes monitoring) [1–3]. Such techniques as fluorescence spectroscopy, near infrared spectroscopy, Raman spectroscopy, chemiluminescence, and liquid chromatography–mass spectroscopy have been applied for the determination of H_2O_2 [4–7]. However, most of these measurements showed their own disadvantages as time consuming, complicated in detection or requiring costly facilities, for instance. Meanwhile, the electrochemical sensors have been proven to be sensitive, selective, fast response, ease of use, and cost-effectiveness in detecting such analytes as H_2O_2 [8, 9].

Prussian blue (ferric hexacyanoferrate, PB) has known to be "artificial peroxidase" due to their high catalytic activity and selectivity in detecting H_2O_2 [3, 10]. The

reduced form of PB (also called Prussian white, PW) [11] is able to catalyze the reduction of hydrogen peroxide at a low applied potential (around 0 V vs. Ag/AgCl), which can obstacle a wide range of interferences in practical use [2, 12, 13]. These excellent characteristics of PB towards H_2O_2 detection can be attributed to its peculiar structure. The unit cell of zeolitic structured PB is large enough (102 nm) to promote the low molecular weight molecules (e.g., O_2 and H_2O_2) diffusing through the crystal, once the molecule of H_2O_2 penetrates the PB lattice, it will be located in the center of each vacancy and surrounded by four divalent high spin iron ions, providing a catalytic active cite for H_2O_2 reduction via a four electron reaction [14, 15].

After the first try from Itaya and Neff [16, 17], PB can be successfully deposited on most of the chemical stable electrodes surface (glassy carbon, Au, Pt, Ag, graphite screen, carbon paste, etc.) via various methods such as electrochemical deposition, in situ chemical deposition, and screen print [18–21]. Being a fast and well-controlled technique for confining PB on to electrodes surface, electrodeposition has been utilized in fabricating flexible and stretchable PB-modified sensors [22, 23].

In the present study, we studied the crucial deposition parameter, i.e., the deposition time, for developing a hydrogen peroxide sensor via electrochemical deposition. Mattos et al. [24, 25] had investigated the influence of

related parameters on stability and activation of PB film on glassy carbon electrodes without considering the monitoring performance; some other studies concerned only on the electrode material with fixed deposition parameter. Thus, the crucial data (thickness, microstructure and electrochemical performance, etc.) for PB-modified gold electrodes in this work are still important and fundamental for further fabricating of high sensitive, wide linear range, and long stable sensors regarding the determination of blood glucose.

2 Materials and methods

2.1 Reagents and materials

Ferric chloride ($FeCl_3$), potassium ferricyanide (III) ($K_3Fe(CN)_6$), potassium chloride (KCl), and 30 wt% hydrogen peroxide (H_2O_2) were all purchased form Sinopharm Chemical Reagent Co., Ltd, China. The tested H_2O_2 solution was prepared via diluting 30 wt% H_2O_2 into different molar concentration with a 0.05 M phosphate buffer solution (PBS, containing 0.05 M KH_2PO_4/K_2HPO_4 and 0.1 M KCl in deionized water, pH 6.2). All inorganic salts were obtained at analytically grade.

The gold film, i.e. the working electrode, for electrodeposition of Prussian blue was prepared by magnetron co-sputtering for 200 nm on a silicon wafer with 400 μm in thickness. Before the sputtering of gold film, an adhesive layer of 20 nm Cr was sputtered onto Si wafer to modify the biding quality between gold and Si substrate.

2.2 Electrochemical deposition of Prussian blue

The electrochemical deposition and measurement were conducted using a CS350-type electrochemical workstation (Corrtest Instrument, China) at room temperature (20–23 °C). A three-electrode cell, which comprised a thin platinum wire as counter electrode (CE), a Ag/AgCl electrode as reference electrode (RE), and the gold film as the working electrode (WE), was used as the testing system. Prior to use, the gold film were all washed in alkaline solution, acid solution, acetone, and deionized water in turn.

Afterwards, Prussian blue (PB) was electrochemically deposited onto the gold film electrodes via applying a constant potential of +400 mV (vs. Ag/AgCl) in an aqueous solution comprising 2.5 mM $FeCl_3$ + 2.5 mM $K_3Fe(CN)_6$ + 0.1 M KCl + 0.12 M HCl (pH 0.89) for 10, 40, 120, and 240 s, respectively. In the following sections, the PB-modified electrodes were distinguished by the aforementioned deposition process, for instance, a sample deposited for 10 s was denoted as ME-10 sample.

Then, the PB-modified electrodes were transferred into a supporting electrolyte containing 0.12 M HCl + 0.1 M KCl solution and electrochemically cycled with a scanning rate of 50 mV s^{-1} between −50 mV (vs. Ag/AgCl) and +350 mV (vs. Ag/AgCl) for 40 cycles. After washing with deionized water, the PB-modified electrodes were dried at 100 °C for 1 h and placed into PBS (pH 6.2) by keeping a constant potential of −50 mV (vs. Ag/AgCl) for 600 s, then washed with deionized water and dried.

2.3 Sensor characterization and electrochemically properties

The microstructure of each PB-modified electrode was observed by field emission scanning electron microscopy (FE-SEM) of LEO-1530 type at an acceleration voltage of 5 kV. The PB samples used for SEM observation were all sprayed with Pt powder. Atomic force microscopy (AFM, Asylum Research Cypher, Oxford Instruments Asylum Research, Inc., USA) was used to analyzed the height information of PB film deposited with different time. The cyclic voltammograms (CVs) were conducted from −50 mV (vs. Ag/AgCl) to +350 mV (vs. Ag/AgCl) by various scanning rate in 0.05 M PBS (pH 6.2). The amperometric response of each type of PB-modified electrode was performed in PBS with a mild stirring rate (~ 200 r min^{-1}) at −100 mV (vs. Ag/AgCl) in room temperature (20–23 °C). The electrochemical results of each type of samples were averaged based on at least three parallel specimens from the same depositing procedure. The error bars of the amperometric response of each type of samples were based on the formula of $\sqrt{\frac{1}{n-1}\sum_1^n (x_i - \bar{x})}$, where x_i is the current response of each electrode towards certain concentration of H_2O_2 solution, $\bar{x}$ is the mean value of current response of each electrode towards certain concentration of H_2O_2 solution, n is the electrodes amount for each deposition time, here the value of $n = 3$.

3 Results

3.1 Microstructure of the deposited PB film

The SEM morphologies in Fig. 1 show the PB film deposited with different times. It can be seen that the PB film is mainly composited with PB particles. Some clusters of PB particles are also observed. The size of these particles is increased with the increase in deposition time, such that when the deposition time reaches 240 s, the length of PB particles reaches about 20 nm. In addition, the shape of the PB particle in ME-10 and ME-40 samples is spherical,
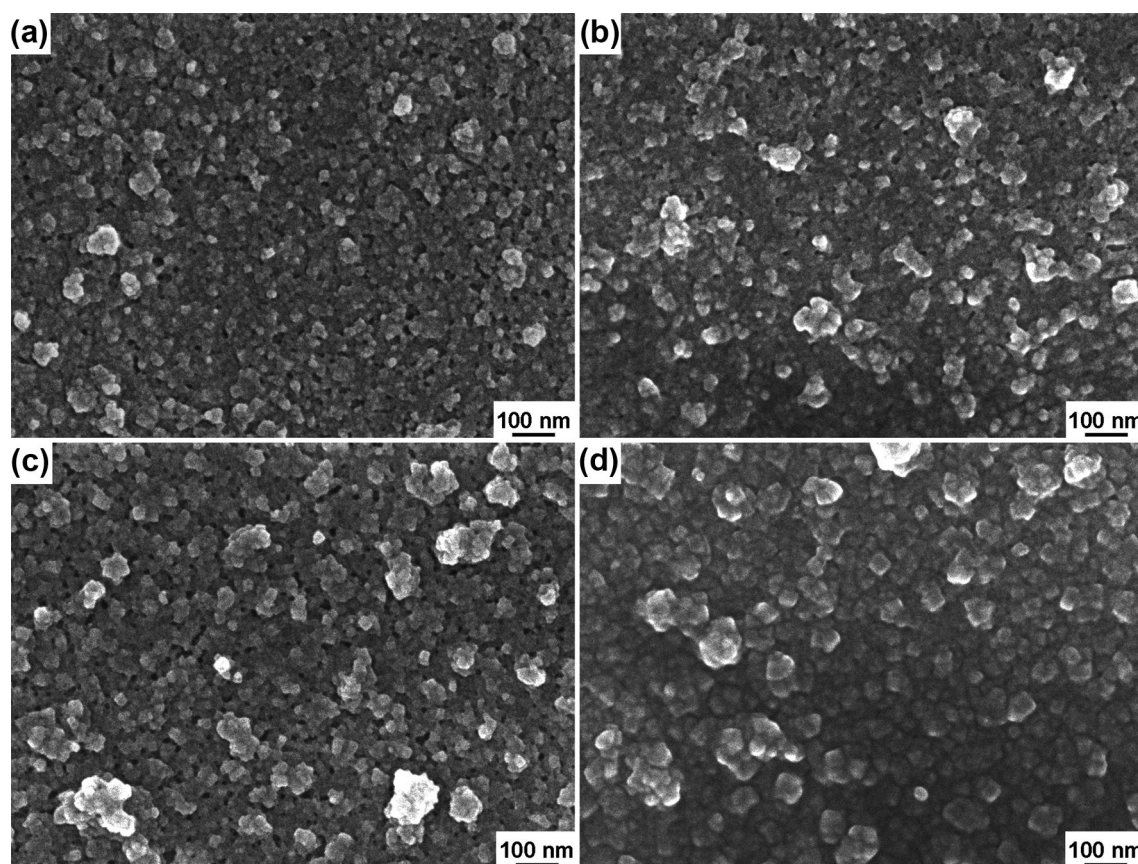
Fig. 1 SEM images of gold electrodes deposited of PB with different times: **a** 10 s, **b** 40 s, **c** 120 s, **d** 240 s

whereas in the PB film deposited for 120 and 240 s. The PB film is mainly consisted with cubic PB crystal.

In order to investigate the change of the PB film thickness in gold film electrodes with different deposition time by AFM, new samples were prepared with the same procedure as other samples used for electrochemical measurements, except that the electrodes used for AFM observation is partially covered by oil ink, which can be dissolved in acetone. After being electrochemically deposited for different times, the AFM samples were ultrasonically cleaned in acetone, where the oil ink was removed and the gold films were all partially covered by PB film. Thus, the thickness of PB film is acquired from the sharp boundary between gold substrate and PB layer. As shown in Fig. 2, the thickness of the PB film is about 30 nm for ME-10 sample, 50 nm for ME-40 sample, 70 nm for ME-120, and 100 nm for ME-240 sample, respectively. This result is in concordance with the study from Mattos [24] that increasing the electrochemically deposition time would lead to an increase in the surface coverage of PB film on the electrode surface, and the electro-catalytic activity of PB film was linearly determined on the surface coverage of PB-modified electrodes.

3.2 Electrochemical characterization of PB film

The quality and electrochemical behavior of the PB-modified electrodes with different deposition time were evaluated by cyclic voltammetry (CV). Figure 3 shows the cyclic voltammograms of the experimental samples recorded under ambient condition with a scan rate of 50 mV s^{-1} in 0.05 M phosphate buffer solution (PBS, pH 6.2), in which a pair of well-defined redox peaks are observed in all PB-modified electrodes, indicating the reversible redox interconversion between Prussian white $\left(\text{PW, } \text{Fe}_4^{3+} \left[\text{Fe}^{2+}(\text{CN})_6 \right]_3 \right)$ and Prussian blue $\left(\text{PB, } \text{K}_4\text{Fe}_4^{3+} \left[\text{Fe}^{2+}(\text{CN})_6 \right]_3 \right)$ [26, 27]. For electrodeposition time ranging from 10 to 120 s, the peak separation (ΔE_p) is about 70 mV. Meanwhile, the ΔE_p value of MP-240 sample reaches 107.94 mV, which indicates an increase of the ohmic resistance [24] and a decrease of reversibility [24] of the PB film after being electrodeposited for 240 s. Moreover, the capacitive current of the experimental PB film is increased with the deposition time from 10 to 40 s; being electrochemically deposited for 120 s, the capacitive current density remains the same as the MP-40 sample. An impressive increase of the capacitive

Fig. 2 Semi contact mode AFM images of **a** ME-10 sample, **b** ME-40 sample, **c** ME-120 sample, and **d** ME-240 sample. (**a1**), (**b1**), (**c1**) and (**d1**) show the height profile of cross section of line 1 in (**a**), line 2 in (**b**), line 3 in (**c**), and line 4 in (**d**), respectively
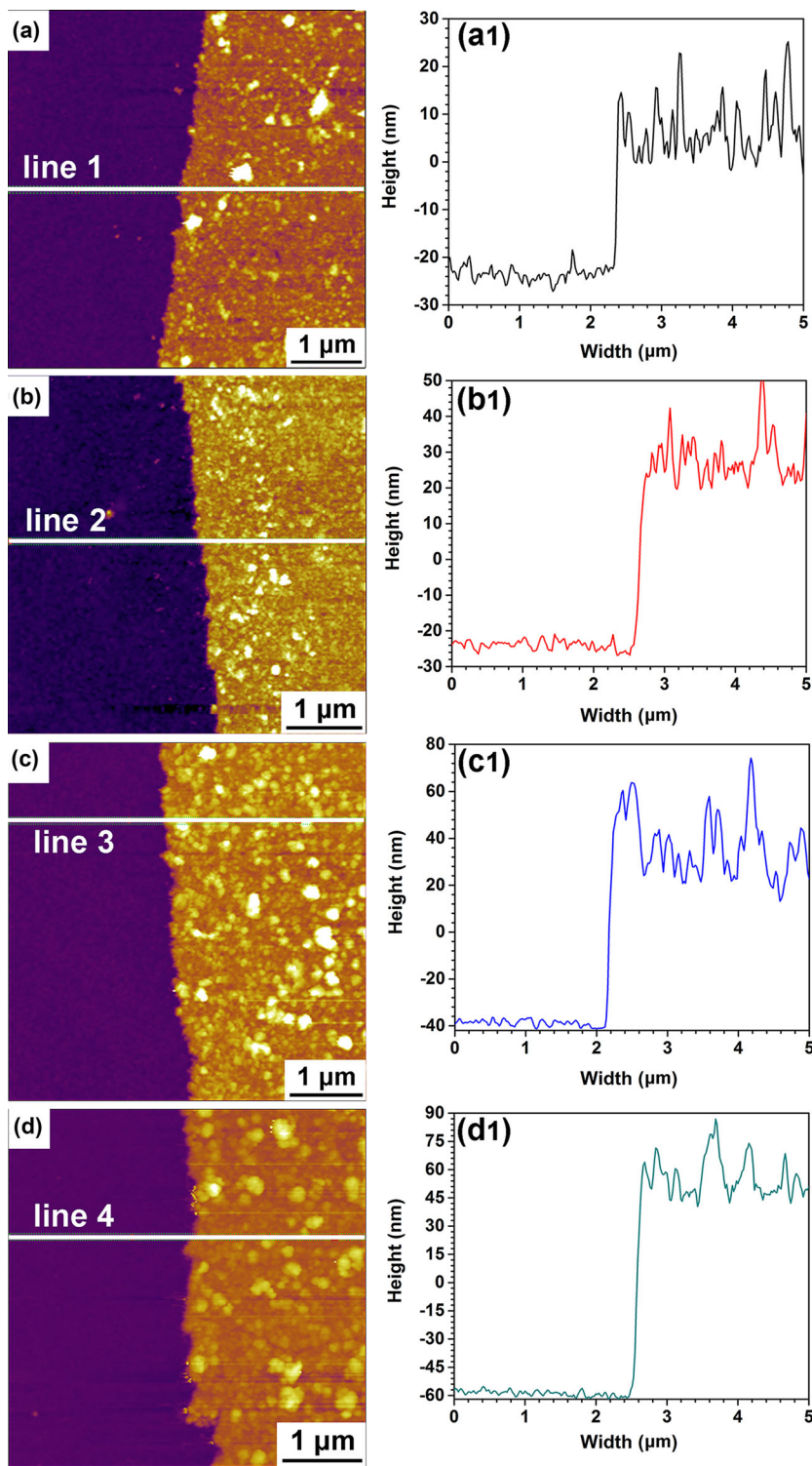
current density is acquired for ME-240 sample, suggesting more electroactive PB was deposited on the gold [25]. Considering the results from thickness analysis (Fig. 2), it can be inferred that the thickness of the PB film would dramatically affect the electro-activity when it reaches about 100 nm. In addition, with larger size of the PB particle (longer deposition time), the exchange of potassium ion (K^+) between PB/solution interfaces would be easier, which consequently improve the electro-activities of obtained PB-modified electrodes.

Figure 4 is the dependency of the peak current of the PB-modified electrodes in 0.05 M PBS (pH 6.2) between

Fig. 3 Cyclic voltammograms of experimental PB-modified electrodes in 0.05 M phosphate buffer (pH 6.2) containing 0.1 M KCl, scan rate: 50 mV s^{-1}
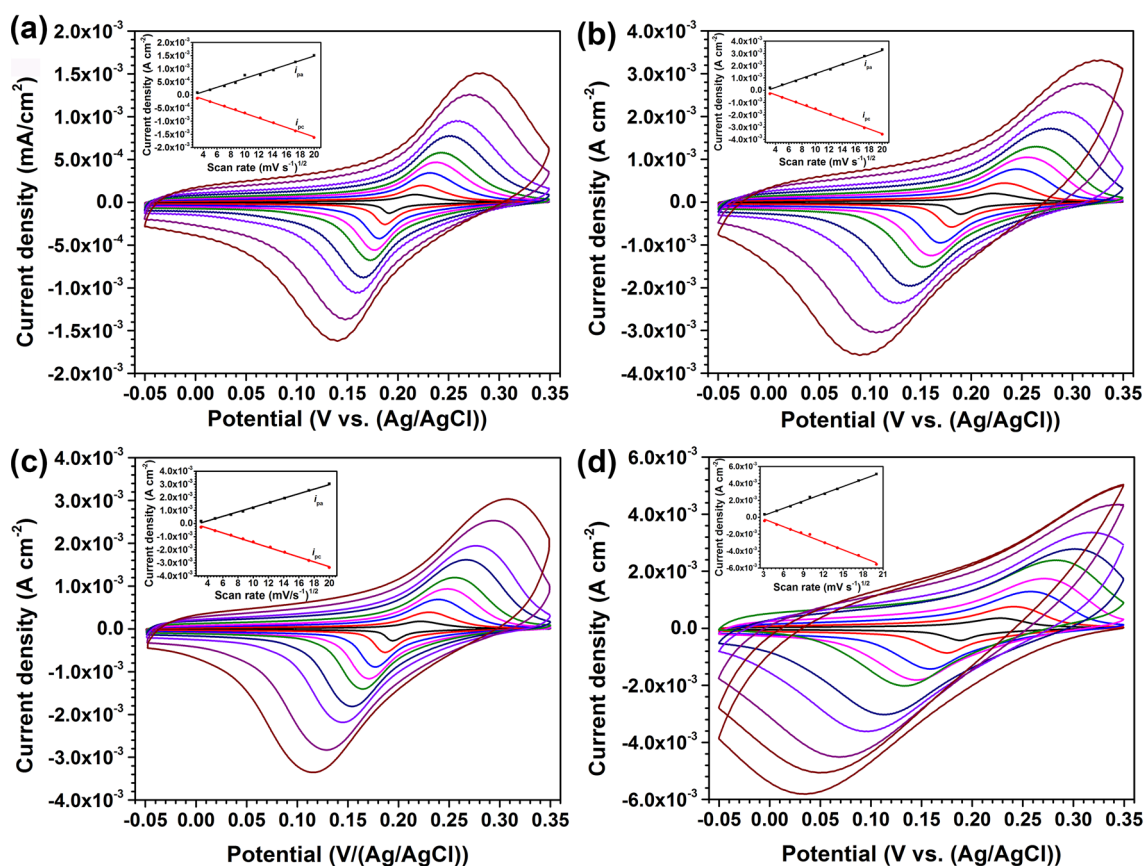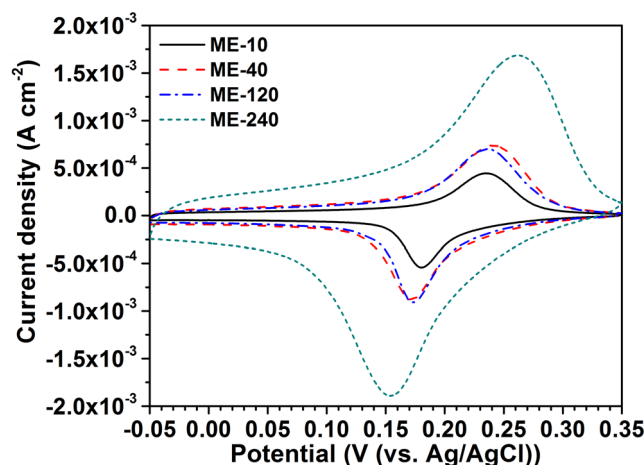

Fig. 4 Cyclic voltammograms of PB-modified electrodes with deposition time of **a** 10 s, **b** 40 s, **c** 120 s, and **d** 240 s. Scan rate varied from 10 to 400 mV s^{-1}, in 0.05 M phosphate buffer with 0.1 M KCl (pH 6.2). *Inset each plot* is the relative anodic and cathodic peak current density versus the square root of scan rate

−5 and 35 mV with the square root of the scan rates ($v^{1/2}$) ranging from 10 to 400 mV s^{-1}. It reveals that all the PB films deposited in this study are in proportional to $v^{1/2}$, indicating the electrochemical process of the system is controlled by diffusion of the counter potassium ion (K$^+$) through the PB lattice [4]. In addition, the potential of cathodic (E_{Pc}) and anodic peaks (E_{Pa}) of these PB-modified

electrodes are shifted along with the increase in scan rate, suggesting that the redox reaction of PB on the electrodes surface is quasi-reversible reaction [28], and the oxidation or reduction properties of the electrodes would be gradually deteriorated.

From Table 1 and Fig. 4, the anodic and cathodic slope values for ME-240 sample (0.28689 and −0.30575

Table 1 Electrochemical parameters from cyclic voltammograms, both stationary scan rate of 50 mV s^{-1} and variational scan rate from 10 to 400 mV s^{-1}

Electrode	Slope (mA cm^{-2})/(mV s^{-1})$^{1/2}$	i_{pa} (50 mV s^{-1}) (mA cm^{-2})	i_{pc} (50 mV s^{-1}) (mA cm^{-2})	ΔE (50 mV s^{-1}) (mV)
ME-10	0.09	0.45	−0.54	54.23
ME-40	0.19	0.74	−0.88	70.40
ME-120	0.18	0.70	−0.91	65.17
ME-240	0.29	1.67	−1.89	107.94

(mA mV s^{-1})$^{1/2}$, respectively) are larger than those of other samples. The slope values of ME-40 and ME-120 samples are slightly different, but still larger than those of the ME-10 sample. According to Randles–Savcik equation [28], the relation between peak current density (i_P) and diffusion coefficient (D) can be summarized as follow:

$$i_P = 2.69 \times n^{3/2} \cdot D^{1/2} \cdot v^{1/2} \cdot A \cdot c, \tag{1}$$

where i_P is the peak current density, n is the number of electrons, D is the diffusion coefficient, v is the scan rates, A is the area of electrodes and c is the concentration. Considering the fact that n is 4, A and c is constant in the measurement procedure, i_P would be proportional to $D^{1/2} \cdot v^{1/2}$. Thus, for diffusion-controlled process, $D^{1/2}$ is proportional to the slop of $i_P - v^{1/2}$ curve ($di_p/dv^{1/2}$) [29]. In this study, increasing the deposition time from 10 to 40 s could improve the diffusion process on electrode surface, but a further increase in time to 120 s cannot further improve that. When the deposition time reaches 240 s, the obtained PB film possesses the highest diffusion coefficient, and thus is much easier for such electron transducers as K$^+$ to enter and leave in the PB lattice.

3.3 Amperometric detection of H$_2$O$_2$

The applied potential at the working electrodes in this study is estimated from other literature [20, 21] as −100 mV (vs. Ag/AgCl). Amperometric response of the experimental PB-modified electrodes towards H$_2$O$_2$ was conducted in 0.05 M phosphate buffer containing 0.1 M KCl (pH 6.2) under mildly stirring (220 r min^{-1} for the magnetic rotor). The results of the chronoamperometry measurements were recorded after successive addition of H$_2$O$_2$ solution with different concentration, and the sensor calibration was performed by plotting the chronoamperometric currents versus H$_2$O$_2$ concentration.

As shown in Fig. 5a, the amperometric response of the ME-40 sample is larger than other samples and the linear relation of the experimental samples is increased with the increase in deposition time. The sensitivities of the sensors are acquired via the slope of the calibration curve (Fig. 5b, S/N = 3). It is noted that the sensitivity of ME-10 sample

(204 mA cm^{-2} M^{-1}, in Table 2) is the worst among all the experimental modified electrodes. With the increase in deposition time, the detecting sensitivity reached the maximum value of 341 mA cm^{-2} M^{-1} for ME-40 sample, then decreased to 282 mA cm^{-2} M^{-1} when the deposition time continuously increased to 240 s. The linear relation of the sensor, in contrast, is increased with the increase in deposition time, and the highest linear range is acquired by ME-240 sample (5 μM–4.5 mM). It has been pointed out that a thinner Prussian blue layer can provide better sensitivity [23]; however, according to our experiments, the thickness of PB layer on Au film electrodes must reached a certain value (50 nm for instance) to acquire better detecting sensitivity. Moreover, the linear range of the PB-modified Au electrode would be determined by the thickness of the PB layer. Considering the results form Figs. 3 and 4, it can be inferred that the linear range for the PB-modified electrodes could be related to the exchange of electron transducers between PB lattice and solution surface. For instance, with a thicker layer, more electroactive PB particle on the ME-240 sample can improve the mobility of K$^+$ among PB lattice. In addition, comparing with several earlier works listed in Table 2, the ME-40 sensor exhibits lower LOD and higher sensitivity. The liner range of current samples (except ME-10 sample) are all better than G-rGO-PB, Nafion-PBNPs-GE and NEA/PB electrodes [21, 30, 31], especially the linear range of ME-240 sample is as high as the work form Cinti [4], which is the highest value acquired from PB-modified electrodes. The results thus indicate that the PB-modified electrode produced by electrodepositing on magnetron co-sputtering gold film with certain deposition time is able to achieve a good balance between excellent analytical properties and utility range.

3.4 Stability and reproducibility of the experimental sensors

The operational stability of hydrogen peroxide sensor is of great importance for their application in continuous monitoring. It is well known that the operational stability of PB-modified sensor is decreased by the thermodynamic instability of the reduced form of PB (Prussian white) and
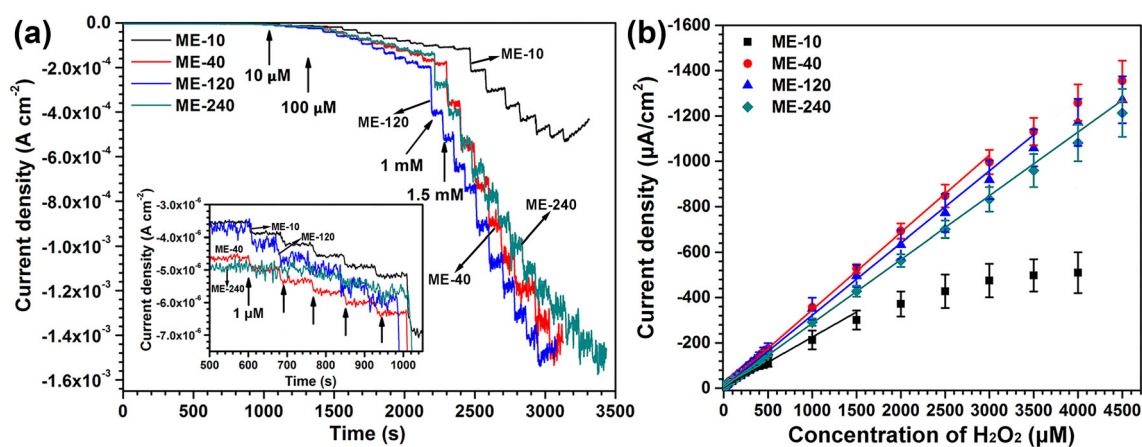
Fig. 5 **a** Amperometric response of the experimental sensors with the successive additions of H_2O_2 in 0.05 M phosphate buffer solution with 0.1 M KCl (pH 6.2). **b** The corresponding calibration curves for H_2O_2 detection. *Inset* (**a**) is the raw amperometric responding data from 1 to 5 μM H_2O_2

Table 2 Comparison of electrochemical behavior of the experimental sensors for H_2O_2 detection

Modified electrode	Linear range (mM)	Sensitivity (mA cm^{-2} M^{-1})	LOD (μM)	Degradation slope (μA min^{-1} cm^{-2})	Stability degree after 1000 cycles (%)	Reference
PBNPs-SPE	10^{-3}–4.5	762	0.2	–	–	[4]
G-rGO-PB	1.6×10^{-3}–0.07	1500	0.5	–	–	[21]
Nafion-PBNPs-GE	2×10^{-3}–0.14	138	1	–	–	[30]
NEA/PB	10^{-5}–1	60	0.01	–	–	[31]
ME-10	10^{-3}–1.0	223	0.2	3.57	66.37	This work
ME-40	10^{-3}–3.0	341	1	1.55	75.65	This work
ME-120	10^{-3}–3.5	318	0.02	1.22	74.85	This work
ME-240	3×10^{-5}–4.5	281	0.01	1.16	78.49	This work

SPE screen printed electrode, *GE* graphite electrode, *GC* glassy carbon electrode, *PBNPs* Prussian blue nano-particles, *NEA* nanoelectrode array, *G-rGO-PB* glucose-oxidized PB particle on reduced graphene oxide sheet

the dissolving of PB polycrystalline caused by hydroxyl ion, which is the product of H_2O_2 reduction [32]. In this study, the operational stability of experimental samples is measured by means of "hydrogen peroxide reduction" [33]. Namely, the test was operated by immersing PB-modified electrode as working electrode (WE) into a stirred batch of PBS with 0.1 M KCl, then a potential of −100 mV was applied on the WE for 10 min to obtain a stable responding current. Afterwards, H_2O_2 solution with certain concentration was injected into the PBS, to obtain a 1 mM concentration of hydrogen peroxide in tested phosphonate buffer solution. The test was terminated when the responding current density decreased −0.1 mA cm^{-2} than the responding current of the injecting point, so the degradation of the responding current density of experimental sensors can be recorded and the slope of the degradation curve could be an indication for evaluating the operational stability of tested sensors.

Similar study was carried out by Borisova [32] and Talagaeva [33] in 0.1 and 1 mM H_2O_2 solution,

respectively. As shown in Fig. 6, the responding current of ME-10 shows a rather fast decay of response after ∼5 - min. With the increase in deposition time, the PB-modified sensors after depositing for 40, 120, and 240 s remained their highest activity at a constant level for about 20 min, which is 2.5 time times greater than the screen printed PB/GC electrode in 0.1 mM H_2O_2 [32] and 10 times higher than PB/Pt electrode in 1 mM H_2O_2 [33]. The slopes from degradation curves (with the unit of mA min^{-1} cm^{-2}) of ME-10, ME-40, ME-120 and ME-240 samples are 3.57×10^{-3}, 1.55×10^{-3}, 1.21×10^{-3} and 1.16×10^{-3}, respectively. In addition, we also measured the stability of experimental sensors via CVs for 1000 cycles. The stability degree of each sample was based on the area ratio of per 100th cycle to initial cycle of the cyclic voltammograms [33, 34]. It can be seen from Fig. 7 and Table 2 that the stability degree of experimental electrodes after 1000 cycles is also increased with the increase in deposition time, indicating that thicker layer of PB film possesses stronger binding with the gold electrode. Comparing to the
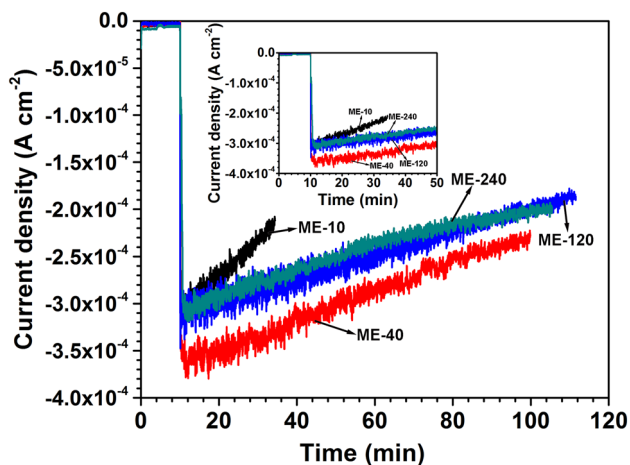
Fig. 6 Current response of experimental PB-modified sensors to stirred flow of 1 mM H_2O_2 in 0.05 M phosphate solution with 0.1 M KCl, PH 6.2, stir rate of 200 r min^{-1}. Inset is the detail data of current response during the early 50 min

results from Talagaeva [33], the stability of PB film on ME-40, ME-120 and ME-240 sample is greater than that of the PB film on ITO-coated GC electrode (deteriorated to nearly 58% after only 500 cycle of CV measurements), and almost the same as the composite Prussian blue–

polypyrrole electrode during the first 1000 cycle (decreased only 12% after 1000 cycle of CV measurements).

The repeatability of the sensor performance, i.e., the storage stability, with each thickness was established by measuring the amperometric response of the electrodes to 1 mM H_2O_2 solution for 5 days and storing the tested electrodes in drying cabinet after each test. The current response for ME-10, ME-40, ME-120, and ME-240 sample respectively remained 75, 89, 90 and 93% of the initial current density after 5 days. The repeatability of inter-electrode was estimated by the ratio between mean squared error and mean value of the current density of three different electrodes in 1 mM H_2O_2 solution. The values of standard deviation for ME-10, ME-40, ME-120 and ME-240 samples are 20, 17, 10, and 5%, respectively. It is worth noting that the results from performance repeatability of tested electrodes are related to the stability test, which showed the same trends that with longer depositing time, the reproducibility of the ME-240 sample would be enhanced. In addition, the stability and reproducibility of ME-10 sample is rather low, and the decrease of stabilities and reproducibility among ME-40, ME-120 and ME-240 samples are slight either in measurement of H_2O_2 electroreduction, the test of CVs ($\sim$5%) or test of
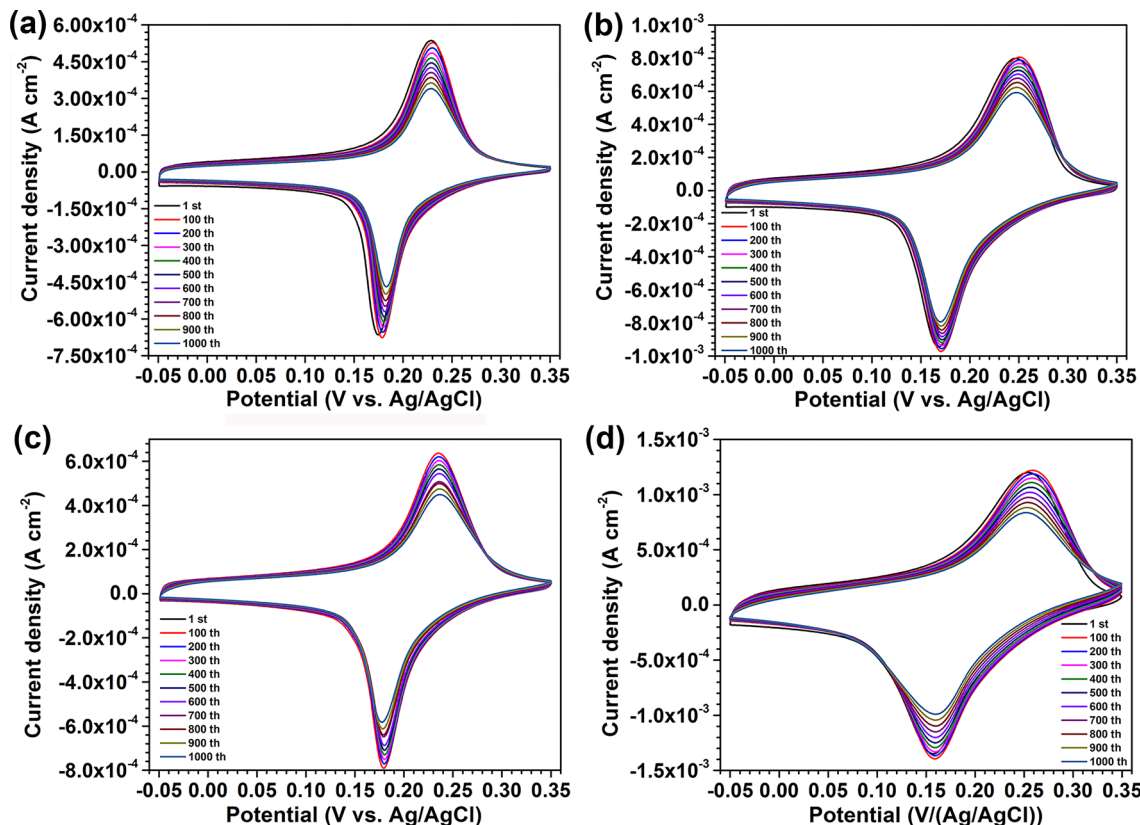

Fig. 7 Repeated cyclic voltammograms of **a** ME-10, **b** ME-40, **c** ME-120, and **d** ME-240 electrodes for 1000 cycles in 0.05 M phosphate buffer solution with 0.1 M KCl (pH 6.2)

reproducibility, suggesting that the thickness of PB film on sensor surface must reach a critical value (50 nm in this work) to acquire necessary working performance.

4 Discussion

The deposition time dramatically affects the microstructure and thickness of the PB film deposited on the gold film. As the deposition time increases, the PB film is constructed by larger cubic particles, and the thickness of PB film is also increased. It reveals in this study that the electrochemical process of the PB-modified electrode is controlled by diffusion of the counter potassium ion (K^+). With larger particle size and film thickness, the ME-240 electrode possesses the highest diffusion coefficient and the widest linear range of which in H_2O_2 amperometric measurements (Fig. 8).

Even though some researchers pointed out that thinner PB layer could provide better sensitivity, our founding shows the thinnest PB layer obtained after being deposited for 10 s exhibits the worst response sensitivity and operational stability. When the deposition time reaches 40 s, ME-40 electrode obtains the highest sensitivity, showing that only when the thickness of PB layer reaches a critical value (50 nm for instance), the exchange of K^+ through PB/solution can be accelerated due to a better diffusion process. As shown in SEM and AFM images, the size of the PB particles for ME-10 and ME-40 samples is nearly the same, and the thickness of ME-40 sample is thicker than ME-10 sample but thinner than ME-120 and ME-240 samples. Considering the fact that the surface area of PB-modified electrode is higher when the particles are smaller which enhances the sensitivity, it turns out that the

thickness and particle size of PB film both determine the sensitivity of the electrodes: smaller particle size offers a higher surface area for PB-modified electrode which enhances the sensitivity, but if the thickness of PB layer is thinner than a critical value (50 nm for instance), the sensitivity of the sensor would be harmed due to the fewer amount of electroactive PB particles that were deposited on electrode surface, which lead to lower response between current density and H_2O_2 concentration. In contrast, a thicker PB layer possesses a larger amount of electroactive PB particles; however, their particle size is larger and the surface area of the PB film is smaller, which would deteriorate the electrochemical action rate and decrease the sensitivity of PB-modified electrode.

5 Conclusions

Electrochemical deposition is an effective method to produce PB-modified gold electrode, which is a promising transducer for selective low-potential detection of hydrogen peroxide. When deposition time reached 240 s, the PB particle size and film thickness, respectively, reached about 20 and 100 nm, which obtain the widest linear range in H_2O_2 amperometric measurements and the best operational stability among all the electrodes. Meanwhile, the best detecting sensitivity is obtained by the electrode deposited for 40 s. It therefore can be concluded that electrodepositing for 240 s would produce the PB-modified electrode with good balance among excellent analytic performance, low cost production, and long-time stability.

References

1. Chen W, Cai S, Ren Q-Q, Wen W, Zhao Y-D (2012) Recent advances in electrochemical sensing for hydrogen peroxide: a review. Analyst 137(1):49–58. doi:10.1039/C1AN15738H
2. Ricci F, Palleschi G (2005) Sensor and biosensor preparation, optimisation and applications of Prussian blue modified electrodes. Biosens Bioelectron 21(3):389–407. doi:10.1016/j.bios
3. Jaffari SA, Turner APF (1997) Novel hexacyanoferrate(III) modified graphite disc electrodes and their application in enzyme electrodes—part I. Biosens Bioelectron 12(1):1–9
4. Cinti S, Arduini F, Moscone D, Palleschi G, Killard A (2014) Development of a hydrogen peroxide sensor based on screen-printed electrodes modified with inkjet-printed Prussian blue nanoparticles. Sensors 14(8):14222–14234
5. Gomes A, Fernandes E, Lima JLFC (2005) Fluorescence probes used for detection of reactive oxygen species. J Biochem Biophys Methods 65(2–3):45–80
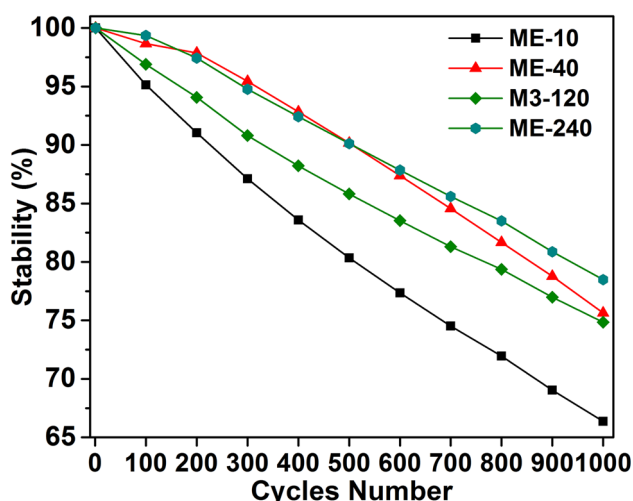
Fig. 8 Stability degree variation of the experimental sensors derived from repeated CVs for 1000 cycle (Fig. 7)

6. Nogueira RFP, Oliveira MC, Paterlini WC (2005) Simple and fast spectrophotometric determination of H2O2 in photo-Fenton reactions using metavanadate. Talanta 66(1):86–91. doi:10.1016/j.talanta

7. Hanaoka S, Lin J-M, Yamada M (2001) Chemiluminescent flow sensor for H2O2 based on the decomposition of H2O2 catalyzed by cobalt(II)-ethanolamine complex immobilized on resin. Anal Chim Acta 426(1):57–64

8. Agnihotry SA, Singh P, Joshi AG, Singh DP, Sood KN, Shivaprasad SM (2006) Electrodeposited Prussian blue films: annealing effect. Electrochim Acta 51(20):4291–4301

9. Omura A, Tanaka H, Kurihara M, Sakamoto M, Kawamoto T (2009) Electrochemical control of the elution property of Prussian blue nanoparticle thin films: mechanism and applications. Phys Chem Chem Phys 11(44):10500–10505. doi:10.1039/B912004A

10. Karyakin AA, Gitelmacher OV, Karyakina EE (1994) A high-sensitive glucose amperometric biosensor based on Prussian Blue modified electrodes. Anal Lett 27(15):2861–2869. doi:10.1080/00032719408000297

11. Keggin J, Miles F (1936) Structures and formulae of the Prussian blues and related compounds. Nature 137(7):577–578

12. Karyakin AA, Karyakina EE, Gorton L (1996) Prussian-Blue-based amperometric biosensors in flow-injection analysis. Talanta 43(9):1597–1606. doi:10.1016/0039-9140(96)01909-1

13. Palleschi G, Ali Nabi Rahni M, Lubrano GJ, Ngwainbi JN, Guilbault GG (1986) A study of interferences in glucose measurements in blood by hydrogen peroxide based glucose probes. Anal Biochem 159(1):114–121. doi:10.1016/0003-2697(86)90315-5

14. Karyakin AA, Karyakina EE, Gorton L (2000) Amperometric biosensor for glutamate using prussian blue-based "artificial peroxidase" as a transducer for hydrogen peroxide. Anal Chem 72(7):1720–1723. doi:10.1021/ac990801o

15. Ludi A, Güdel HU (1973) Structural chemistry of polynuclear transition metal cyanides. Inorganic chemistry. Springer, Berlin, pp 1–21

16. Neff VD (1978) Electrochemical oxidation and reduction of thin films of Prussian blue. J Electrochem Soc 125(6):886–887. doi:10.1149/1.2131575

17. Itaya K, Uchida I, Neff VD (1986) Electrochemistry of polynuclear transition metal cyanides: Prussian blue and its analogues. Acc Chem Res 19(6):162–168. doi:10.1021/ar00126a001

18. Bandodkar AJ, Jia W, Yardımcı C, Wang X, Ramirez J, Wang J (2015) Tattoo-based noninvasive glucose monitoring: a proof-of-concept study. Anal Chem 87(1):394–398. doi:10.1021/ac504300n

19. Zhang D, Wang K, Sun DC, Xia XH, Chen HY (2003) Ultrathin layers of densely packed prussian blue nanoclusters prepared from a ferricyanide solution. Chem Mater 15(22):4163–4165. doi:10.1021/cm034594r

20. Fu G, Yue X, Dai Z (2011) Glucose biosensor based on covalent immobilization of enzyme in sol–gel composite film combined with Prussian blue/carbon nanotubes hybrid. Biosens Bioelectron 26(9):3973–3976. doi:10.1016/j.bios.2011.03.007

21. Zhang M, Hou C, Halder A, Ulstrup J, Chi Q (2017) Interlocked graphene–Prussian blue hybrid composites enable multifunctional electrochemical applications. Biosens Bioelectron 89(1):570–577. doi:10.1016/j.bios.2016.02.044

22. Kim D-H, Viventi J, Amsden JJ, Xiao J, Vigeland L, Kim Y-S, Blanco JA, Panilaitis B, Frechette ES, Contreras D, Kaplan DL, Omenetto FG, Huang Y, Hwang K-C, Zakin MR, Litt B, Rogers JA (2010) Dissolvable films of silk fibroin for ultrathin conformal bio-integrated electronics. Nat Mater 9(6):511–517

23. Gao W, Emaminejad S, Nyein HYY, Challa S, Chen K, Peck A, Fahad HM, Ota H, Shiraki H, Kiriya D, Lien D-H, Brooks GA, Davis RW, Javey A (2016) Fully integrated wearable sensor arrays for multiplexed in situ perspiration analysis. Nature 529(7587):509–514. doi:10.1038/nature16521

24. Mattos ILd, Gorton L, Ruzgas T, Karyakin AA (2000) Sensor for hydrogen peroxide based on Prussian blue modified electrode: improvement of the operational stability. Anal Sci 16(8):795–798. doi:10.2116/analsci.16.795

25. de Mattos IL, Gorton L, Ruzgas T (2003) Sensor and biosensor based on Prussian Blue modified gold and platinum screen printed electrodes. Biosens Bioelectron 18(2–3):193–200

26. Chen A, Rogers EI, Compton RG (2009) Abrasive stripping voltammetry in room temperature ionic liquids. Electroanal 21(1):29–35. doi:10.1002/elan.200804401

27. Ahmadalinezhad A, Kafi AKM, Chen A (2009) Glucose biosensing based on the highly efficient immobilization of glucose oxidase on a Prussian blue modified nanostructured Au surface. Electrochem Commun 11(10):2048–2051

28. Bard A, Faulkner L (2001) Electrochemical methods: fundamentals and applications. Wiley, New York

29. Khan R, Dhayal M (2008) Electrochemical studies of novel chitosan/TiO2 bioactive electrode for biosensing application. Electrochem Commun 10(2):263–267. doi:10.1016/j.elecom.2007.12.001

30. Haghighi B, Hamidi H, Gorton L (2010) Electrochemical behavior and application of Prussian blue nanoparticle modified graphite electrode. Sensor Actuat B-Chem 147(1):270–276. doi:10.1016/j.snb.2010.03.020

31. Karyakin AA, Puganova EA, Budashov IA, Kurochkin IN, Karyakina EE, Levchenko VA, Matveyenko VN, Varfolomeyev SD (2004) Prussian blue based nanoelectrode arrays for H2O2 detection. Anal Chem 76(2):474–478. doi:10.1021/ac034859l

32. Borisova AV, Karyakina EE, Cosnier S, Karyakin AA (2009) Current-free deposition of Prussian blue with organic polymers: towards improved stability and mass production of the advanced hydrogen peroxide transducer. Electroanal 21(3–5):409–414. doi:10.1002/elan.200804408

33. Talagaeva NV, Zolotukhina EV, Bezverkhyy I, Konev DV, Lacroute Y, Maksimova EY, Koryakin SL, Vorotyntsev MA (2015) Stability of Prussian blue–polypyrrole (PB/PPy) composite films synthesized via one-step redox-reaction procedure. J Solid State Electrochem 19(9):2701–2709. doi:10.1007/s10008-015-2951-3

34. Lin Y, Hu L, Yin L, Guo L (2015) Electrochemical glucose biosensor with improved performance based on the use of glucose oxidase and Prussian Blue incorporated into a thin film of self-polymerized dopamine. Sensor Actuat B-Chem 210:513–518. doi:10.1016/j.snb.2014.12.107